Set up of a double pass AOM system for an ion trap experiment

Lukas Möller
Supervisor: Dr. Thomas Lutz
Professor: Prof. Dr. Jonathan Home
TIQI-Group, ETH Zürich

October 30, 2018

Abstract

Acousto-optic modulators are used to control amplitude and frequency of laser pulses. The beam path for a double-pass geometry of an acousto-optic modulator was planned and set up. The efficiency of the setup was studied using a testing acousto-optic modulator. A diffraction efficiency of 65% (single-pass) could be achieved. In addition the initial laser output beam was investigated. An elliptic beam shape with a beam diameter of 650 nm in horizontal and 400 nm in vertical direction was measured.

Contents

1 Introduction

Quantum computing is a fast growing topic. The qubit is not limited to states 1 and 0 as for the conventional bit used in today's computers, but can be any superposition thereof. That way the amount of stored information in a single qubit is much larger than in a single bit. Quantum systems use qubits to perform algorithms much faster and with a lower energy need than conventional computers. However, the necessary experimental capabilities to implement qubits are still to be accomplished. Trapped ions are leading candidates for the practical implementation of quantum information processing. In the TIQI-group at ETH Zürich, beryllium and calcium ions are investigated; also in combination with optical cavities. Laser light is used to cool and control the ions which is a prerequisite for trapping. For that purpose one has to be able to precisely control the wavelength and the timing of laser pulses.
A possibility to control the wavelength of a laser within a small range are acousto-optic modulators (AOM). In Ch. 2 a brief explanation of the functionality of AOMs and the physical concepts on which they rely on is given. However, the focus of this semester thesis was on the experimental work.
During the thesis a laser path for the AOM was planned. After completing some initial trouble

shooting and characterization of the pump laser the optics were set up. The thesis is concluded with the key measurements to specify the functionality of the AOM in this setup.

2 Theory of acousto-optic modulators

The idea to scatter light on acoustic waves in material was developed in 1922 [1]. The first application was realized shortly thereafter. The invention of lasers enhanced the interest in acousto-optic modulation as it can be used for precise beam control [8].

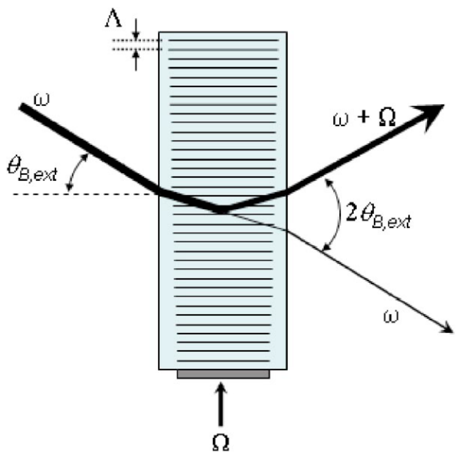

Figure 1: Schematic drawing of a laser beam passing through an acousto-optic medium driven by an RF voltage with frequency Ω. Source: Donley et. al. [2]

In a good approximation the process can be described as photon diffraction on a grating induced by a spatially modulated refractive index. Via a transducer the RF signal creates density waves, which move inside the medium and induce the changes in the refractive index [2]. For the diffraction process inside a medium with long interaction range the picture of Bragg treating it as photon-phonon scattering is sufficient [8]. A photon can absorb a phonon in a first-order process. Using the energy-momentum relations one finds for frequency and wave vector of the scattered photon

$$\omega_d = \omega_i + \Omega \tag{1}$$
$$k_d = k_i + \kappa, \tag{2}$$

with the frequencies ω and Ω and the wave vectors k and κ of the photon and phonon respectively. The subscript i indicates the incoming photon and d a deflected photon. Neglecting the frequency shift, one finds the relation for the diffraction angle (Bragg angle Θ_B)

$$\sin \Theta_B = \frac{\kappa}{2k_i}. \tag{3}$$

this relation is called Bragg's Law or Bragg condition. In an acousto-optic modulator, the deflection efficiency for first order is maximized when (3) is fulfilled [5]. Note: to get the correct angle for the input and output beam $\Theta_{B,ext}$, one has to take into account the diffraction of light on the boarder between the acousto-optic active medium and air.

3 Design of a double-pass AOM

3.1 Characterizing the pump laser

The necessary laser light is supplied by a M2-laser at a wavelength of $\lambda = 794\,\mathrm{nm}$, which is doubled to get the correct wavelength of $\lambda = 397\,\mathrm{nm}$ for the transition $S_{\frac{1}{2}} \rightarrow P_{\frac{1}{2}}$ of $^{40}Ca^{+}$. The initial output power is around $P = 2000\,\mathrm{mW}$. During the day some power fluctuations were observed. A warm up period of at least two hours is recommended.

This output power is too high for our purpose. For that reason a half-wave plate together with a Glan-Taylor polarizer (calcite, extinction ratio 100000:1 [7]) was put into the beam line to be able to vary the power. Experimentally, a much smaller extinction ratio was observed as one can see from Fig. 2 with a minimum power of $P_{min} = 28\,\text{mW}$. The reason for that is that the polarization of the light going into the prism was not strictly linear. With an additional quarter-wave plate inserted into the beam path the minimum power could be reduced to $P = 0.9\,\text{mW}$, which is convenient for the alignment process. Later a power of around $P = 200\,\text{mW}$ is needed to control ions. This can be achieved using the half-wave plate.

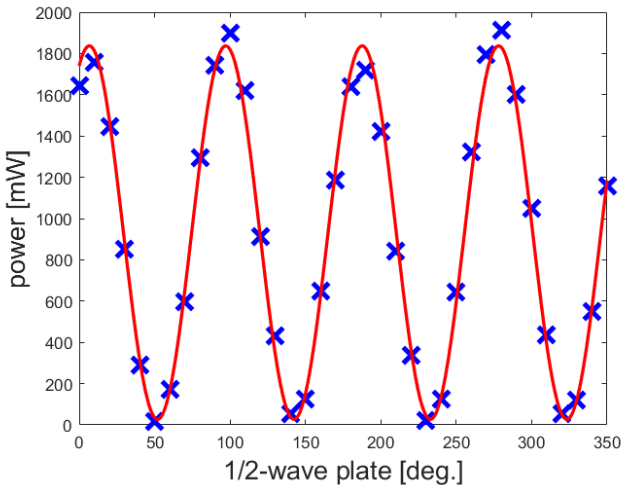

Figure 2: Laser power measured after the polarizer as a function of the angle of the half-wave plate without a quarter-wave plate.

Furthermore, the collimation of the laser beam was examined. Already after propagating a short distance in free space the beam size grew noticeably and the beam shape became visible. Due to an unexpected beam shape it was investigated further with a beam profiler right after the polarizer. The measured beam shapes are shown in Fig. 3. It can be assumed that the beam is not altered with respect to the beam shape after leaving the M2 laser. An ideal beam would be of Gaussian shape with the same width in all directions. This is not the case for the laser here. During the first two hours after turning on the laser a slow increase of the diameter was observed. The beam is stable after running it for a few hours. However, it remains elliptical with an considerably larger horizontal beam diameter of 650 nm in comparison to the diameter in vertical direction of 400 nm.

3.2 Setting up a double-pass AOM geometry

The setup was planned as a double-pass geometry for the AOM similar to that described in [2]. This has the advantage that the frequency shift is doubled. In addition, the shift of diffraction angle that is acquired upon changing the RF frequency in the medium is cancelled. Thus, the optics will not have to be realigned for a new frequency. After the double-pass through the AOM the deflected beam has to be separated from the initial beam. This is accomplished by reflecting the beam with a prism resulting in a vertical shift between incoming and outgoing beam. Due to this spatial separation a mirror can be put into the beam path in such a way that only the deflected beam is caught by it. The whole setup is on a breadboard such that it is mobile.
The AOM that will be used in the final experiment is the model 1250C-829A by ISOMET[1]. For our wavelength a diffraction efficiency of more than 85% and a zeroth to first order beam separation of 25.1 mrad is stated in the data sheet [4]. For testing of the setup the model ASM-802B8 by Intraaction Corp. (Polytec)[2] featuring a diffraction efficiency of 85% and a beam separation of

[1]Specifications of AOM 1250C-829A: Standard A/R wavelengths: $360 - 420\,\text{nm}$, $442 - 488\,\text{nm}$, interaction medium: tellurium dioxide, active aperture: 0.45 mm, centre frequency: 260 260MHz, RF bandwidth: 100 MHz [4]

[2]Specifications of AOM ASM-802B8: Standard A/R wavelengths: $300 - 400\,\text{nm}$, $442 - 488\,\text{nm}$, interaction medium: UV grade fused silica, active aperture: 2 mm, centre frequency: 80 260MHz, RF bandwidth: 15 MHz [6]

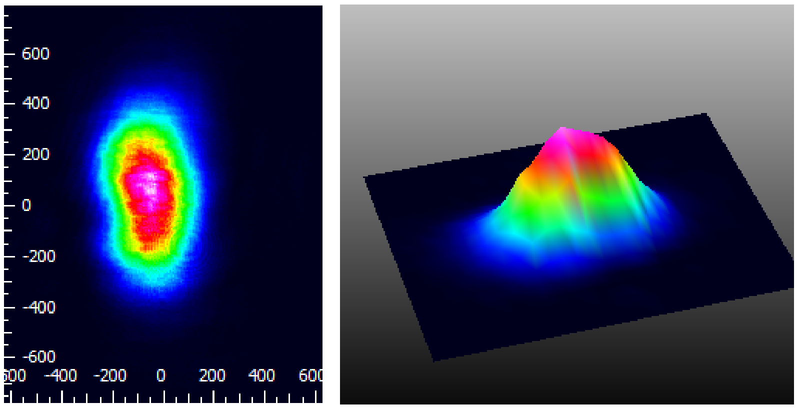

(a) (b)

Figure 3: Beam shape of the initial beam after the GT polarizer measured with the beam profiler BC106N-VIS. Red indicates regions of high power with descending power for yellow to green to blue to black. The dimensions are in μm

4.8 mrad was utilized.
As the diameter of the output beam of the M2 laser (see Ch. 3.1) is larger than the active aperture of the AOM 1250C-829A it has to be decreased for an optimal performance of the AOM. Two possibilites were considered, requiring that the beam is still collimated after passing the AOM. On the one hand, one can use a lens in front and one after the AOM with the focal point inside the active medium to achieve this. On the other hand, a telescope can be put in front of the AOM. We decided to use a telescope due to the higher deflection efficiency [2]. To decrease the beam diameter by a factor of 3, lenses with focal lengths of $f_1 = 75$ mm and $f_2 = -25$ mm were chosen as we intended to build a very compact system.

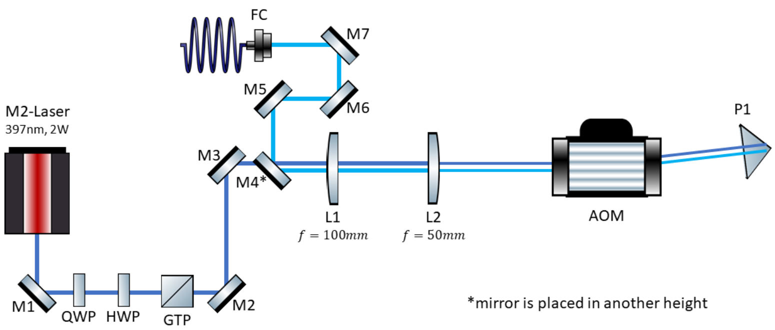

Figure 4: Scheme of the initially planned setup for the double-pass geometry. The beam emerges from the laser source. For clarity the returning beam after the AOM is colored in light blue to be distinguished from the initial beam in dark blue. The laser is coupled in to a fiber by a fiber collimator (FC). L_i are lenses, M_i are mirrors and P1 is a prism. Optical components designed by Alexander Franzen [3].

The thoughts above led to the setup displayed in Fig. 4. After the pass through the AOM the laser is coupled into a fiber. While setting up the optical components as planned in Fig. 4, some problems with handling the laser beam occured:
As mentioned in Ch. 3.1, the beam was not perfectly collimated. This made the placement of the

lenses without a cage system difficult. Additionally, the aberrations resulting from an off-centre passage through a thick lens like the one with $f_2 = -25\,\mathrm{mm}$ are very detrimental to the beam shape, which leads to problems with fiber coupling. This off-centre passage is forced by the separation of initial and reflected beam resulting in worse beam quality regarding beam shape and collimation. To avoid this problem, we decided to switch to another pair of lenses with $f_1 = 100\,\mathrm{mm}$ and $f_2 = 50\,\mathrm{mm}$ mounted in a cage.
Note that the beam separation of the test-AOM is much smaller than with the one that will be used in the end. With the test AOM, free propagation of the laser for a length of 10 cm after the AOM would cause only a separation of $480\,\mu\mathrm{m}$, which is similar to the size of the beam diameter. Thus one needs more space after the AOM to separate zeroth and first order beam. For that reason the setup was modified as can be seen in Fig. 5.

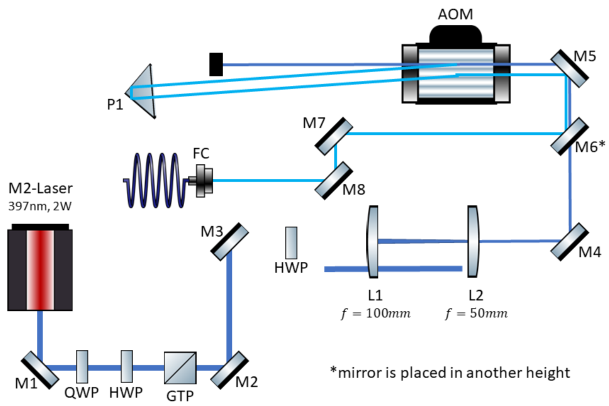

Figure 5: Scheme of the final setup for the double-pass mount of an AOM as it has been built in HPF B 25. The beam emerges from the laser source (M2 laser). For clarity the returning beam after the AOM is colored in light blue to be distinguished from the initial beam in dark blue. The laser is coupled in to a fiber by a fiber collimator (FC). Optical components designed by Alexander Franzen [3].

3.3 Characterizing the efficiency of the setup

3.3.1 Model ASM-802B8

Some characterization measurements were performed to verify the functioning of the setup. Initial alignment led to a diffraction efficiency of 45% (100%$\hat{=}$4 mW) for the first order deflection after a single-pass. The dependence of the AOM deflection efficiency on RF drive power is shown in Fig. 6. For relative RF drive power higher than 50%, a linear dependence of the diffraction efficiency on the RF input power was observed. Normally a saturation is expected for high input power. This was not observed near the specified maximal input power for the AOM.

In addition, the dependence of the diffraction efficiency on the RF frequency was examined. As can be seen in Fig. 7 a maximum occurred at about 87 MHz. Working at this RF frequency and optimizing the beam position and angle again, a diffraction efficiency of 65% was achieved. The setup is working near its specified performance. With further optimization of the position and angle of the beam the predicted efficiency of 85% from the data sheet should be possible.

3.3.2 Model 1250C-829A

The measurements could not be made until now because the AOM did not arrive.

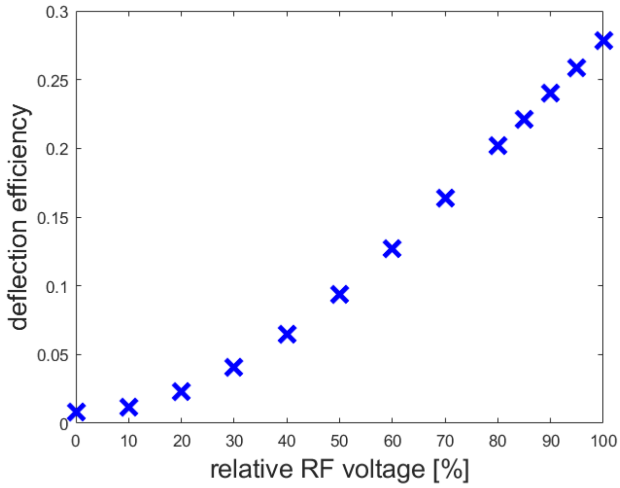

Figure 6: First order deflection efficiency of the AOM as it depends on the relative RF drive voltage for an RF frequency of 80 MHz.

3.3.3 Coupling into fiber

The deflected beam will be coupled into a fiber and guided to the ion trap. The AOM by ISOMET can only handle up to 200mW of power. Therefore it is important to achieve an optimal coupling efficiency. The procedure to couple into fiber requires some fine tuning. Two mirrors in front of the fiber are optimal. That way one has all degrees of freedom. With the mirror right in front of the fiber the angle in vertical and horizontal can be adapted and with the second one the vertical and horizontal position can be changed. One proceeds in three steps:

1. Overlap the laser with a probe laser coming through the fiber from the other end to obtain rough alignment.
2. Move the mirrors to maximize the signal initially.
3. Turn the corresponding screws of both coupling mirrors slightly for either the vertical or horizontal direction in opposite way maximizing the signal. Repeat this step for both directions till the global maximum is reached.

Following the procedure a coupling efficiency of 40% was reached with the setup from Fig. 5 after a short time for optimization. During the setup process an efficiency up to 55% was observed without an AOM. The coupling efficiency is possibly limited by the overlap of the Gaussian mode of the fiber and the laser mode, as the laser mode is not Gaussian and is in size larger than the maximum aperture of the fiber coupler.

4 Outlook

The foundation is built to use the laser in further experiments. The new AOM has still to be characterized when it arrives. Yet it should take only a short time to do the alignment process with it. For further usage the frequency tuning capabilities has to be characterized for the new AOM.

References

[1] Brillouin, Léon. Diffusion de la lumière et des rayons x par un corps transparent homogène - influence de l'agitation thermique. *Ann. Phys.*, 9(17):88–122, 1922.

[2] E. A. Donley, T. P. Heavner, F. Levi, M. O. Tataw, and S. R. Jefferts. Double-pass acousto-optic modulator system. *Review of Scientific Instruments*, 76(6):063112, 2005.

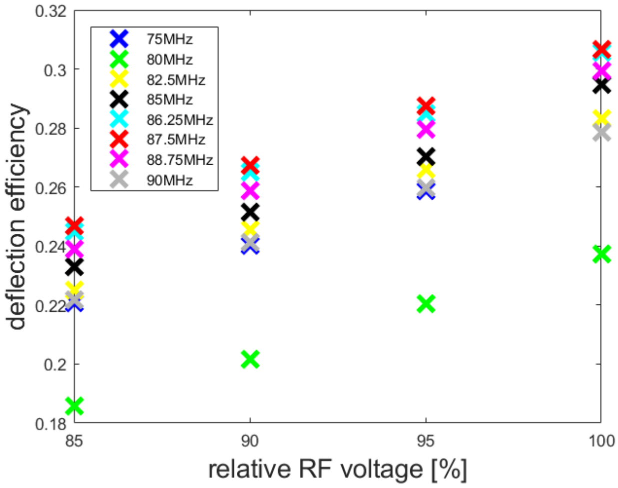

Figure 7: First order deflection efficiency of the AOM as it depends on the relative RF drive voltage for different RF frequencies.

[3] A. Franzen. Component library. http://www.gwoptics.org/ComponentLibrary/.

[4] ISOMET Corp. *1250C-829A Acousto-Optic Modulator*.

[5] ISOMET Corp. *All About Bragg Angle Errors in AO Modulator & Deflector, Application Note AN 1022*.

[6] Polytec GmbH. *MODEL ASM-B SERIES UV ACOUSTO-OPTIC MODULATOR / FREQUENCY SHIFTER*, 2005.

[7] Thorlabs Inc. *GLAN TAYLOR POLARIZER*, 2009.

[8] J. E. H. Young and S.-K. Yao. Design considerations for acousto-optic devices. *Proceedings of the IEEE*, 69(1):54–64, Jan 1981.